Supporting Information

In-situ construction of 3D low-coordinated bismuth nanosheets@Cu nanowires core-shell nanoarchitectures for superior CO_2 electroreduction activity

*Yanjie Hu[1], Dongzhen Lu[1], Weiliang Zhou[1], Xinying Wang, Yunyong Li**

School of Materials and Energy, Guangdong University of Technology, No. 100 Waihuan Xi Road, Guangzhou Higher Education Mega Center, Guangzhou 510006, China

*E-mail: yyli@gdut.edu.cn (Y. Y. Li) Tel: (+8620)-39322570, Fax: (+8620)-39322570.

[1] These authors contributed equally to this work.

Experimental section

***Materials*:** All chemical reagents are directly used without further purification as all chemical regents were of analytical grade. $BiCl_3$ was purchased from Beijing InnoChem Science & Technology Co., Ltd. Dimethyl sulfoxide (DMSO) were purchased from Tianjin Zhiyuan Chemical Reagent Co., Ltd. Sodium hydroxide (NaOH), ammonium persulphate ($(NH_4)_2S_2O_8$), potassium bicarbonate (KHCO3), and sulfuric acid (H_2SO_4) was purchased from Shanghai Aladdin Bio-Chem Technology Co., Ltd. Cu foam was purchased from Bosai Electrochemical Materials Network. Nafion solution was purchased from Shanghai Hesen Electric Co., Ltd. Gaseous CO_2, H_2/Ar, and N_2 were obtained from Guangzhou Shengying Gas Co., Ltd.

***Fabrication of Cu NWs/Cu*:** Firstly, copper hydroxide NWs ($Cu(OH)_2$ NWs/Cu) was prepared by a chemical oxidation method based on previous research. [1, 2] In a typical procedure, a piece of Cu foam (1 cm × 1.5 cm) was immersed into 50 mL of an aqueous containing 1.245 g $(NH_4)_2S_2O_8$ and 5 g NaOH for 20 min. Subsequently, the Cu foam with light blue was washed with deionized water and dried at 60 °C. The as-prepared $Cu(OH)_2$ NWs/Cu was placed in a quartz, and heated in tube furnace at 180 °C in the air for 1h to get copper oxide NWs (CuO NWs/Cu). Finally, the Cu NWs/Cu was obtained by reduction of the CuO NWs/Cu in a forming gas (8% H_2/Ar) at 300 °C for 2h.

***Synthesis of Cu@BiOCl NWs/Cu*:** To grow bismuth oxychloride (BiOCl) *in situ* on Cu NWs/Cu, a piece of Cu NWs/Cu was put into 25 mL of a DMSO solution containing 20 mg $BiCl_3$ for 24 h. Then the Cu@BiOCl NWs/Cu was washed with ethanol for several times and dried at 60 °C to obtain light-yellow Cu@BiOCl NWs/Cu.

***Synthesis of Cu@Bi NWs/Cu*:** *In-situ* preparation of Cu@Bi NWs/Cu was got through electrochemical reduction of Cu@BiOCl NWs/Cu employing in a Metrohm Autolab electrochemical workstation in stand three-electrode configuration with one-chamber. For the cathodic conversion from Cu@BiOCl NWs/Cu to Cu@Bi NWs/Cu, the Cu@BiOCl NWs/Cu, the platinum gauze and Ag/AgCl (saturation) electrode were used as working electrode, as counter electrode and as reference electrode, respectively. After cyclic voltammetry (CV) experiments with the scan rate 50 mV s^{-1} were performed to reduce to Cu@BiOCl NWs/Cu to Cu@Bi NWs/Cu in N_2-saturated 0.1 M $KHCO_3$ aqueous solution from -0.8 V to -1.2 V for 500 cycles. Finally, the black Cu@Bi NWs/Cu was taken out from the electrolyte, washed with deionized and ethanol for several times, respectively, and dried at 60 °C.

***Preparation of working electrodes*:** Typically, commercial Bi powder (2 mg) was dispersed in a solution

consisting of Nafion solution (5 wt%, 20 μL) and isopropanol (240 μL) by ultrasonic treatment for 1 h to form homogeneous Bi catalyst ink. Then, the obtained homogeneous solution is then added dropwise to the Cu NWs/Cu (designated as Bi-Cu NWs/Cu) or Cu foam (designated as Bi/Cu) and then dried at room temperature for 24 h. Cu@Bi NWs/Cu or Cu NWs/Cu was directly used as the working electrode.

***Material characterizations*:** The phase composition and crystallinity of the samples were characterized via the powder X-ray diffraction (XRD) (D8 ADVANCE with Cu Kα (λ = 0.15406 nm)). The microstructures of samples were detected via a scanning electron microscope (SEM, Hitach SU8220), a transmission electron microscopy (TEM) and a high-resolution TEM (HRTEM, FEI Talos F200s). X-ray photoelectron spectroscopy (XPS) (Escalab 250Xi with Al Kα radiation source) was applied to study the surface chemistry of the samples.

***Electrochemical measurements and product analysis*:** All electrochemical data were recorded using PGSTAT302N potentiostat/galvanostat (Metrohm Autolab, Netherlands) with Cu@Bi NWs/Cu, Cu NWs/Cu, Bi-Cu NWs/Cu or Bi/Cu as working electrode, platinum gauze (1 cm × 1 cm) as counter electrode and Ag/AgCl (3.5M KCl) as reference electrode. Linear sweep voltammetry (LSV) curves were conducted with PGSTAT302N potentiostat/galvanostat using the commercial H-cell configuration with a sweep rate of 50 mV/s from -0.03 V to -1.27 V (vs. RHE). Electrochemical impedance spectroscopy (EIS) of Cu@Bi NWs/Cu, Cu NWs/Cu, Bi-Cu NWs/Cu and Bi/Cu were performed at the constant potential mode over a frequency range from 100 kHz to 0.01 Hz with an amplitude of 5 mV. The electrochemical double-layer capacitances (C_{dl}) were recorded via a series of cyclic voltammetry (CV) between 0.3 V to 0.4 V (vs. RHE) with different scan rate in 0.5 M $KHCO_3$. The CO_2RR was performed at normal temperature and pressure using a commercial gas-tight H-type cell with Nafion 117 membrane (Shanghai Hesen Electric Co., Ltd) separating the anode and cathode compartments. 0.5 M $KHCO_3$ was the catholyte, and the anolyte was 0.1 M H_2SO_4 aqueous solution. The catholyte was saturated with CO_2 before the start of the catalytic experiment. The cathode solution was stirred gently to mix better while CO_2 gas passed in at a speed of 50 mL min^{-1}. The cathode solutions were collected at the end of each electrocatalysis, and the liquid products were analyzed qualitatively and quantitatively by ^{1}H-NMR (AVANCE III HD 600MHz).

***Computations*:** The present first principle DFT calculations with the projector augmented wave (PAW) method were performed by Vienna Ab initio Simulation Package (VASP). [3, 4] The exchange-functional is treated using the generalized gradient approximation (GGA) of Perdew-Burke-Ernzerhof (PBE)

functional. [5] The Vaspkit code [6] was used for the post processing of the data, and the energy cutoff for the plane wave basis expansion was set to be 500eV, the Brillouin zone integration was sampled by 2*2*1 point for the Cu (111) surface and Bi (110) surface, 2*3*1 point for Cu-Bi heterojunction, and the force on each atom less than 0.03 eV/Å was set for convergence criterion of geometry relaxation. 15 Å vacuum was added along the z direction in order to avoid the interaction between periodic structures. The self-consistent calculations apply a convergence energy threshold of 10^{-5} eV. The DFT-D3 method was employed to consider the van der Waals interaction. [7] The Gibbs free energy changes for each electrochemical step was calculated by the expression:

$$\Delta G = \Delta E_{DFT} + \Delta ZPE + \int_0^T C_P dT - T\Delta S$$

Where ΔE_{DFT} is the total electronic energy change, ΔZPE is the change of zero-point energy, $\int_0^T C_P dT$ is the change of enthalpic temperature correction, ΔS is the change of entropy, T is the reaction temperature.

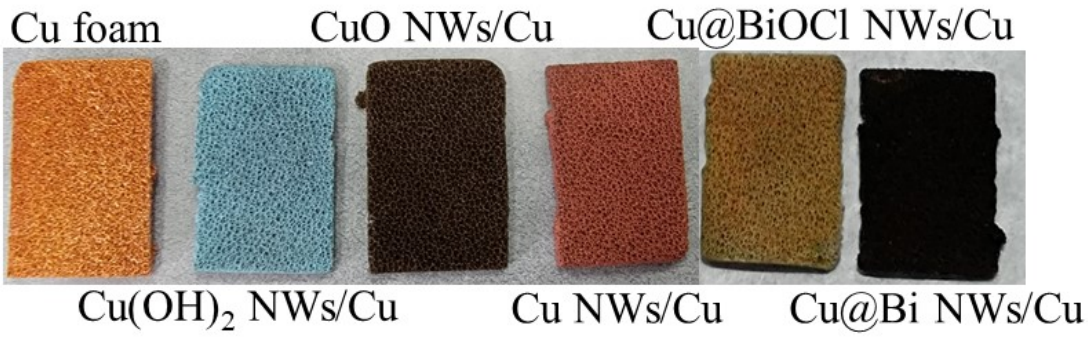

Fig. S1. Optical photographs of Cu foam, $Cu(OH)_2$ NWs/Cu, CuO NWs/Cu, Cu NWs/Cu, BiOCl@Cu NWs/Cu and Bi@Cu NWs/Cu.

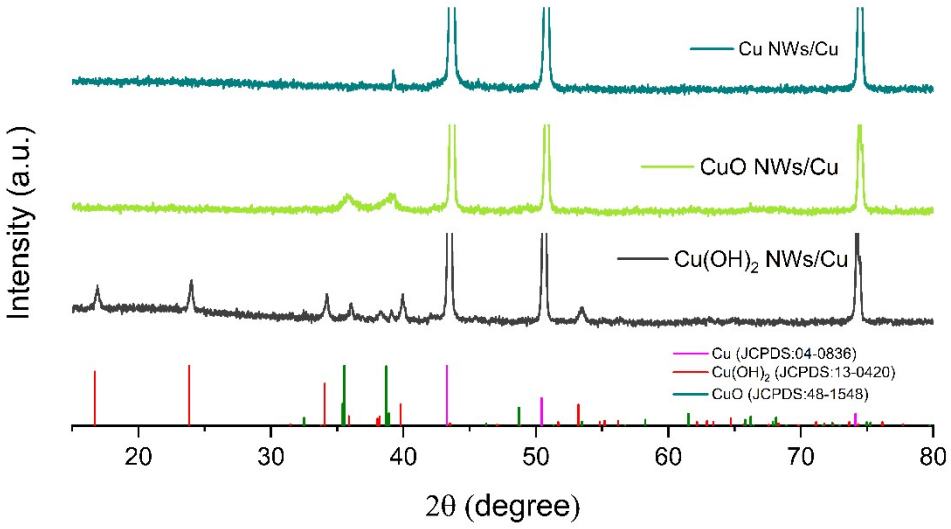

Fig. S2. XRD patterns of $Cu(OH)_2$ NWs/Cu, CuO NWs/Cu and Cu NWs/Cu.

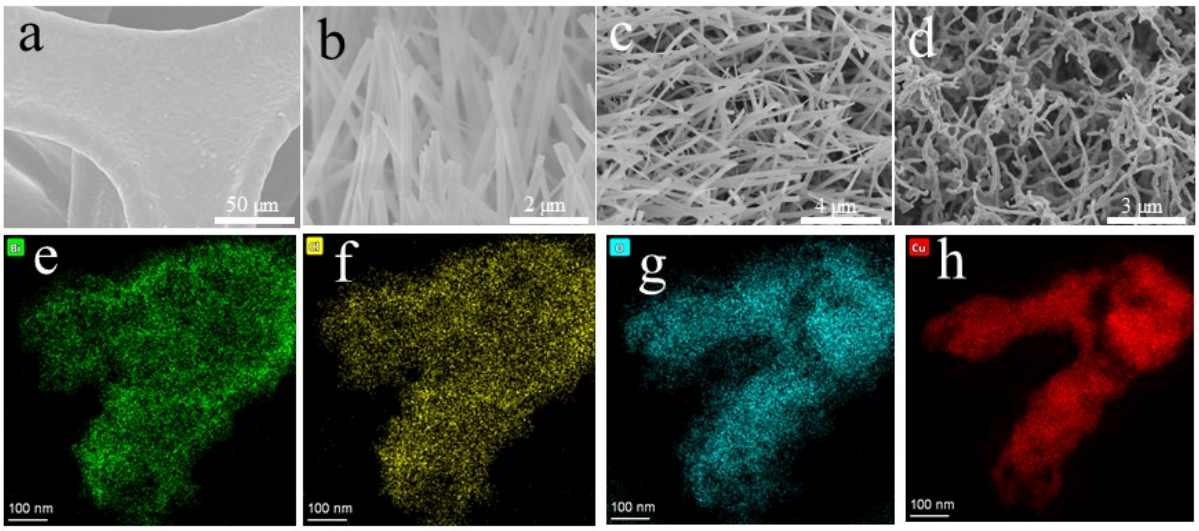

Fig. S3. Characterization of Cu foam, $Cu(OH)_2$ NWs/Cu, CuO NWs/Cu, Cu NWs/Cu and Cu@BiOCl NWs/Cu. SEM image of (a) Cu foam, (b) $Cu(OH)_2$ NWs/Cu, (c) CuO NWs/Cu, (d) Cu NWs/Cu and (e)-(h) EDX elemental mapping of Cu@BiOCl NWs/Cu.

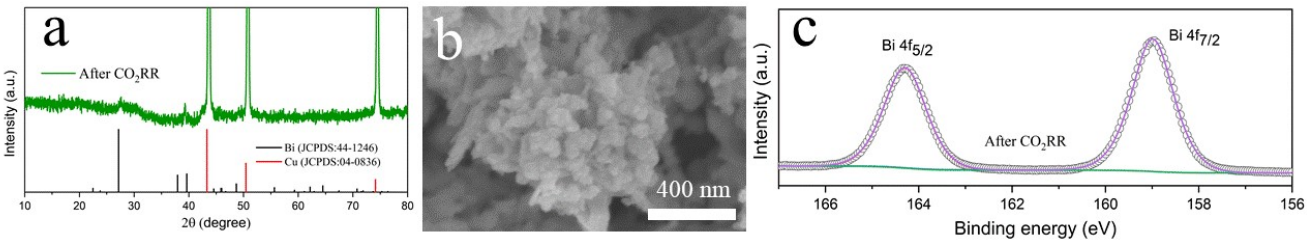

Fig. S4. (a) XRD patterns of Cu@Bi NWs/Cu after CO_2RR; (b) SEM images of Cu@Bi NWs/Cu after CO_2RR; (c) XPS spectra of Cu@Bi NWs/Cu after CO_2RR (The two peaks of Bi 4f can be observed at 159 eV and 164.3 eV.).

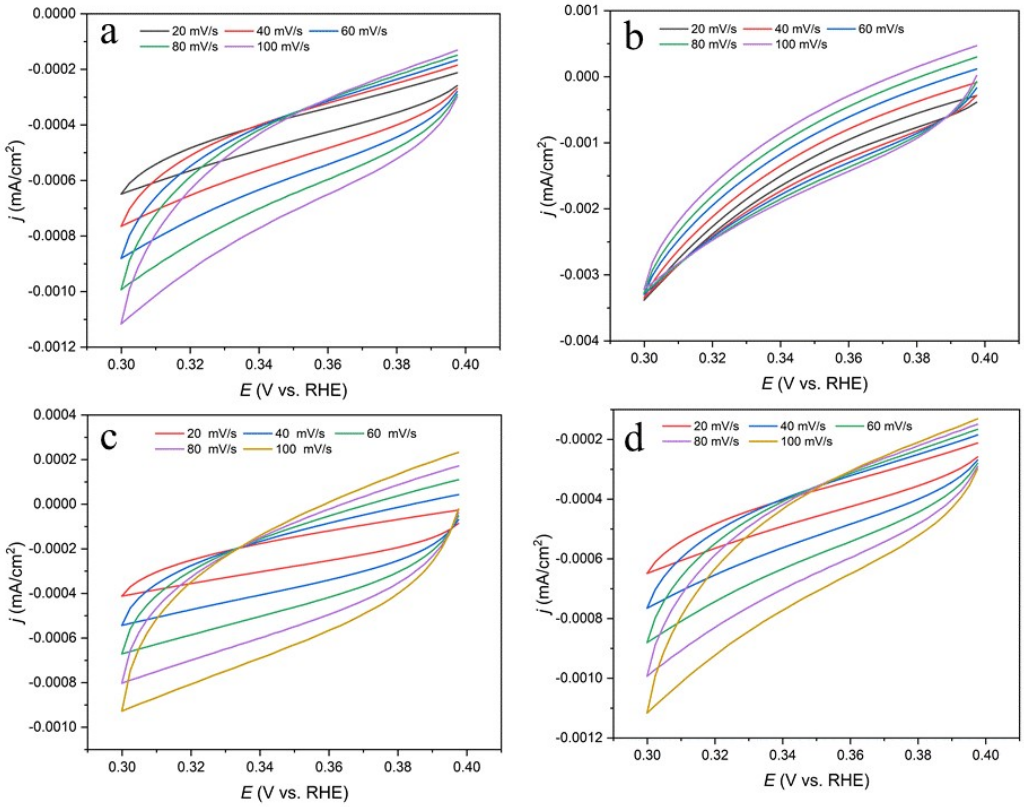

Fig. S5. CVs curves of (a) Cu@Bi NWs/Cu, (b) Cu NWs/Cu, (c) Bi-Cu NWs/Cu, (d) Bi/Cu with scan rates ranging from 20 to 100 $mV \cdot s^{-1}$ in 0.5 M $KHCO_3$.

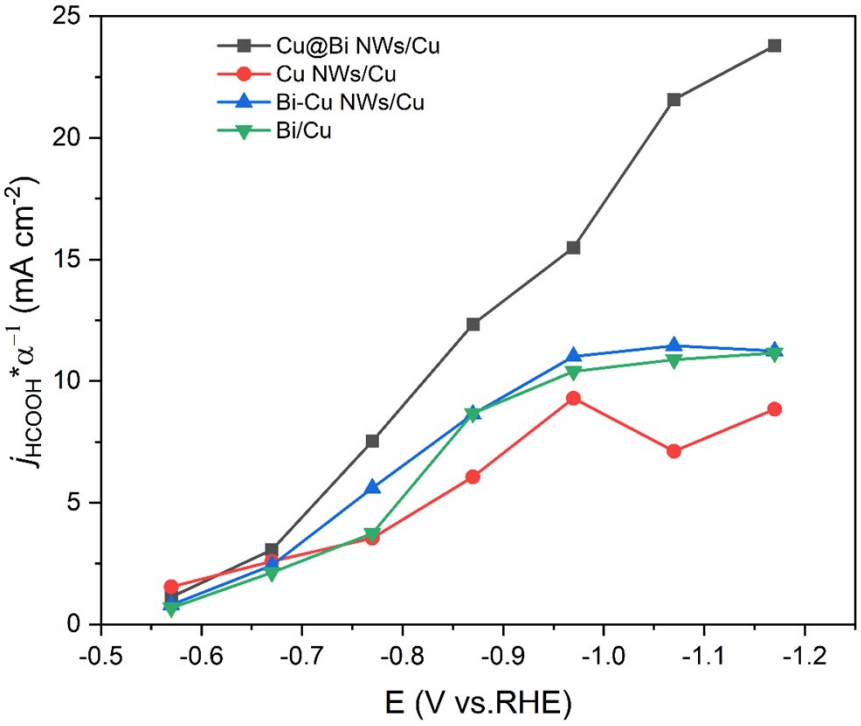

Fig. S6. Partial current density for HCOOH normalized to ECSA of Cu@Bi NWs/Cu, Cu NWs/Cu, Bi-Cu NWs/Cu and Bi/Cu.

Table S1. Comparisons of CO_2RR performance for Cu@Bi NWs/Cu with reported electrocatalysts.

Catalysts	Applied potential (vs. RHE)	j_{total} (mA cm^{-2})	FE_{HCOOH}	References
Bi/Sn	-1.1 V	34.1	91	8
BiOBr	-1.0 V	80	99	9
Bi	-1.18 V	72	100	10
POD-Bi	-1.16 V	57	95	11
SnS/Aminated-C	-0.9 V	52.1	92.6	12
In-Sn core-shell	-1.1 V	46.1	74	13
mesoporous SnO_2 NSs	-0.96 V	51.7	87	14
BiOx/C	-1.23 V	37.8	89.3	15
In_2O_3/InN	-1.59 V	18.6	95	16
Bi/Nafion@Cu	-1.17 V	75.9	95	17
Bi_2S_3-Bi_2O_3	-1.1 V	18.2	93.8	18
Sub-2 nm SnO_2	-1.16 V	15.7	87.3	19
Bi NSs	-1.5 V (vs. SCE)	14.8	95	20
Bi_2O_3 NSs@MCCM	-1.26 V	16.2	93.8	21
Bi-300	-0.9 V	16.7	91.6	22
Bi/CeO_x	-1.3 V	149	92	23
pits-Bi NS	-1.14 V	32.9	95.3	24
BiCu/Cu	-1.2 V	98.2	89.4	25
Bi-Sb	-0.9 V	43.3	95.8	26
Bi-Sn	-1.14 V	111.8	92.1	27
Cu@Bi NWs/Cu	**-1.07 V**	**129**	**98.7**	**This work**
Cu@Bi NWs/Cu	**-1.17 V**	**155.8**	**90.1**	**This work**

Table S2. The Bader charge of D-Bi (110) and Cu (111)@D-Bi (110) respectively.

Atomic number	D-Bi (110)	Cu (111)@D-Bi (110)
1	15.06	15.12
2	15.02	15.04
3	15.02	15.08
4	14.99	15.00
5	15.01	15.08

References

1 L. Yu, H. Zhou, J. Sun, F. Qin, F. Yu, J. Bao, Y. Yu, S. Chen and Z. Ren, *Energy Environ. Sci.*, 2017, **10**, 1820-1827.

2 D. Raciti, K. J. Livi and C. Wang, *Nano Lett.*, 2015, **15**, 6829-6835.

3 P. E. Blochl, *Phys. Rev. B*, 1994, **50**, 17953-17979.

4 G. Kresse and J. Furthmuller, *Phys. Rev. B*, 1996, **54**, 11169-11186.

5 J. Perdew, J. Chevary, S. Vosko, K Jackson, M Pederson, D. Singh, C. Fiolhais, *Phys. Rev. B* 1992, **46**, 11.

6 V. Wang, N. Xu, J. C. Liu, G. Tang and W. T. Geng, *Comput. Phys. Commun.*, 2021, **267**, 108033.

7 S. Grimme, J. Antony, S. Ehrlich and H. Krieg, *J. Chem. Phys.*, 2010, **132**, 154104.

8 Y. Xing, X. Kong, X. Guo, Y. Liu, Q. Li, Y. Zhang, Y. Sheng, X. Yang, Z. Geng and J. Zeng, *Adv. Sci.*, 2020, **7**, 1902989.

9 F. P. Garcia de Arquer, O. S. Bushuyev, P. De Luna, C. T. Dinh, A. Seifitokaldani, M. I. Saidaminov, C. S. Tan, L. N. Quan, A. Proppe, M. G. Kibria, S. O. Kelley, D. Sinton and E. H. Sargent, *Adv. Mater.*, 2018, **30**, e1802858.

10 C. Cao, D. D. Ma, J. F. Gu, X. Xie, G. Zeng, X. Li, S. G. Han, Q. L. Zhu, X. T. Wu and Q. Xu, *Angew. Chem. Int.*, 2020, **59**, 15014-15020.

11 S. He, F. Ni, Y. Ji, L. Wang, Y. Wen, H. Bai, G. Liu, Y. Zhang, Y. Li, B. Zhang and H. Peng, *Angew. Chem. Int.*, 2018, **57**, 16114-16119.

12 Z. Chen, X. Zhang, M. Jiao, K. Mou, X. Zhang and L. Liu, *Adv. Energy Mater.*, 2020, **10**, 1903664.

13 J. Wang, S. Ning, M. Luo, D. Xiang, W. Chen, X. Kang, Z. Jiang and S. Chen, *Appl. Catal. B*, 2021, **288**, 119979.

14 F. Li, L. Chen, G. P. Knowles, D. R. MacFarlane and J. Zhang, *Angew. Chem. Int.*, 2017, **56**, 505-509.

15 X. H. Zhao, Q. S. Chen, D. H. Zhuo, J. Lu, Z. N. Xu, C. M. Wang, J. X. Tang, S. G. Sun and G. C. Guo, *Electrochim. Acta*, 2021, **367**, 137478.

16 X. Zhao, M. Huang, B. Deng, K. Li, F. Li and F. Dong, *Chem. Eng. J.*, 2022, **437**, 135114.

17 S. Chang, Y. Xuan, J. Duan and K. Zhang, *Appl. Catal. B*, 2022, **306**, 121135.

18 P. F. Sui, C. Xu, M. N. Zhu, S. Liu, Q. Liu and J. L. Luo, *Small*, 2022, **18**, e2105682.

19 S. Liu, J. Xiao, X. Lu, J. Wang, X. Wang, X. (David) Lou, *Angew. Chem. Int. Ed.*, 58 (2019) 8499-8503.

20 N. Han, Y. Wang, H. Yang, J. Deng, J. Wu, Y. Li and Y. Li, *Nature Commun.*, 2018, **9**, 1320.

21 S. Liu, X. F. Lu, J. Xiao, X. Wang and X. W. D. Lou, *Angew. Chem. Int.*, 2019, **58**, 13828-13833.

22 L. Yi, J. Chen, P. Shao, J. Huang, X. Peng, J. Li, G. Wang, C. Zhang and Z. Wen, *Angew. Chem. Int.*, 2020, **59**, 20112-20119.

23 Y. Duan, Y. Zhou, Z. Yu, D. Liu, Z. Wen, J. Yan, Q. Jiang, *Angew. Chem. Int. Ed.*, 2021, **60**, 8798-8802.

24 Y. Yuan, Q. Wang, Y. Qiao, X. Chen, Z. Yang, W. Lai, T. Chen, G. Zhang, H. Duan, M. Liu, H. *Adv. Energy Mater.*, **2022**, 2200970.

25 B. Liu, Y. Xie, X. Wang, C. Gao, Z. Chen, J.Wu, H. Meng, Z. Song, S. Du, Z. Ren, *Appl. Catal. B*, 2022, **301**, 120781.

26 W. Yang, C. Si, Y. Zhao, Q. Wei, G. Jia, G. Cheng, J. Qin, Z. Zhang, *Appl. Catal. B*, 2022, **316**, 121619.

27 B. Ren, G. Wen, R. Gao, D. Luo, Z. Zhang, W. Qiu, Q. Ma, X. Wang, Y. Cui, L. Ricardez-Sandoval, A. Yu, Z. Chen, *Nat. Commun.*, 2022, **13**, 2486.